63-9713.4-12

SPRING SEPARATION OF SPACECRAFT

by

D. H. Mitchell
G. D. Palmer

EM 13-10 2319-6038-TU-000

April 1963

Approved Millard V. Barton

Millard V. Barton, Director
Engineering Mechanics Laboratory

SPACE TECHNOLOGY LABORATORIES, INC.
A Subsidiary of Thompson Ramo Wooldridge Inc.
One Space Park • Redondo Beach, California

ABSTRACT

29723

The detailed equations of motion for a spacecraft separating from a final rocket stage or another spacecraft by means of separation springs have been derived and programmed for solution on the IBM 7090 digital computer.

This report shows how the equations were derived, which parameters are significant, and how the program can be used to compute tipoff errors for actual spring separation system design.

Author

This work was performed under Contract No. NAS5-899 for Goddard Space Flight Center, National Aeronautics and Space Administration, Greenbelt, Maryland.

CONTENTS

ILLUSTRATIONS

1. INTRODUCTION

For the OGO and 823 programs, the Dynamics Department of STL has studied in detail the problem of separating spacecraft from their final booster stage and from each other by the use of precision helical compression springs. Analyses have been performed to verify that these separation springs provide an adequate relative velocity between the two bodies, but do not introduce excessive tipoff angles and angular rates.

The basic equations of motion used for these studies have been programmed for the IBM 7090 digital computer. The use of this program has greatly reduced the computation time required to look at the importance of each of the many parameters which bear on the problem.

Gross dynamic effects of a two-body separation can be easily found by "hand" solutions of relatively simple impulse-momentum equations. Solutions such as this have proved quite adequate for determining preliminary estimates of required separation spring stroke length, spring rates, etc. When the precise motion that may be imparted to the spacecraft by this type of separation needs to be known, however, a more detailed solution is required.

This report outlines such a solution. It has been simplified, however, since the typical spring separation of a spacecraft from a final rocket stage produces tipoff angles which are usually much less than 1 degree and tipoff rates on the order of 1 to 2 deg/sec. Since these are very small, assumptions can be made which greatly decrease the complexity of the equations of motion.

Solution by digital computer makes it possible to study variations in the large number of weight and dimensional parameters produced by manufacturing and assembly tolerances.

2. DYNAMIC MODEL AND COORDINATE SYSTEMS

The basic model of the spacecraft separation problem consists of two rigid bodies, clamped together before separation is initiated, forced apart by up to four separation springs, and, finally, completely separated. All motion of both bodies is limited to a single plane. Each body translates along two axes and rotates in this plane. The mass and inertia properties of each body are considered to be time invariant.

Essentially two dynamic models have been used. The first, shown in Figure 1, represents the geometry to be used in obtaining the initial mated-body accelerations, due to residual thrust of the final rocket stage, which set many of the initial conditions of the problem.

The dynamic model shown in Figure 2 is used to define the coordinate system of each body from the "equilibrium" position. The bodies are in the "equilibrium" position when the total axial and lateral separation spring forces cancel out the respective inertia forces in the initial acceleration field. The equations of motion of each body have been written using these coordinates.

3. INITIAL MATED-BODY CONDITIONS

Besides any arbitrary initial conditions on the two bodies there will be conditions at $t = 0$ (when the springs are released) imposed by residual thrust in the final rocket stage. These conditions are determined by use of the model as shown in Figure 1, where the residual thrust force is broken into two components, T_x and T_y, parallel and perpendicular, respectively, to the final stage centerline. Each component is assumed to be constant during the separation sequence.

When the two bodies are mated the composite cg will be as shown in Figure 1. In many cases the composite cg and moment of inertia of the two bodies are not known but must be calculated from the individual stage parameters. Considering static moments about a point on the separation plane in Figure 1 to find $\ell_{\overline{X}}$,

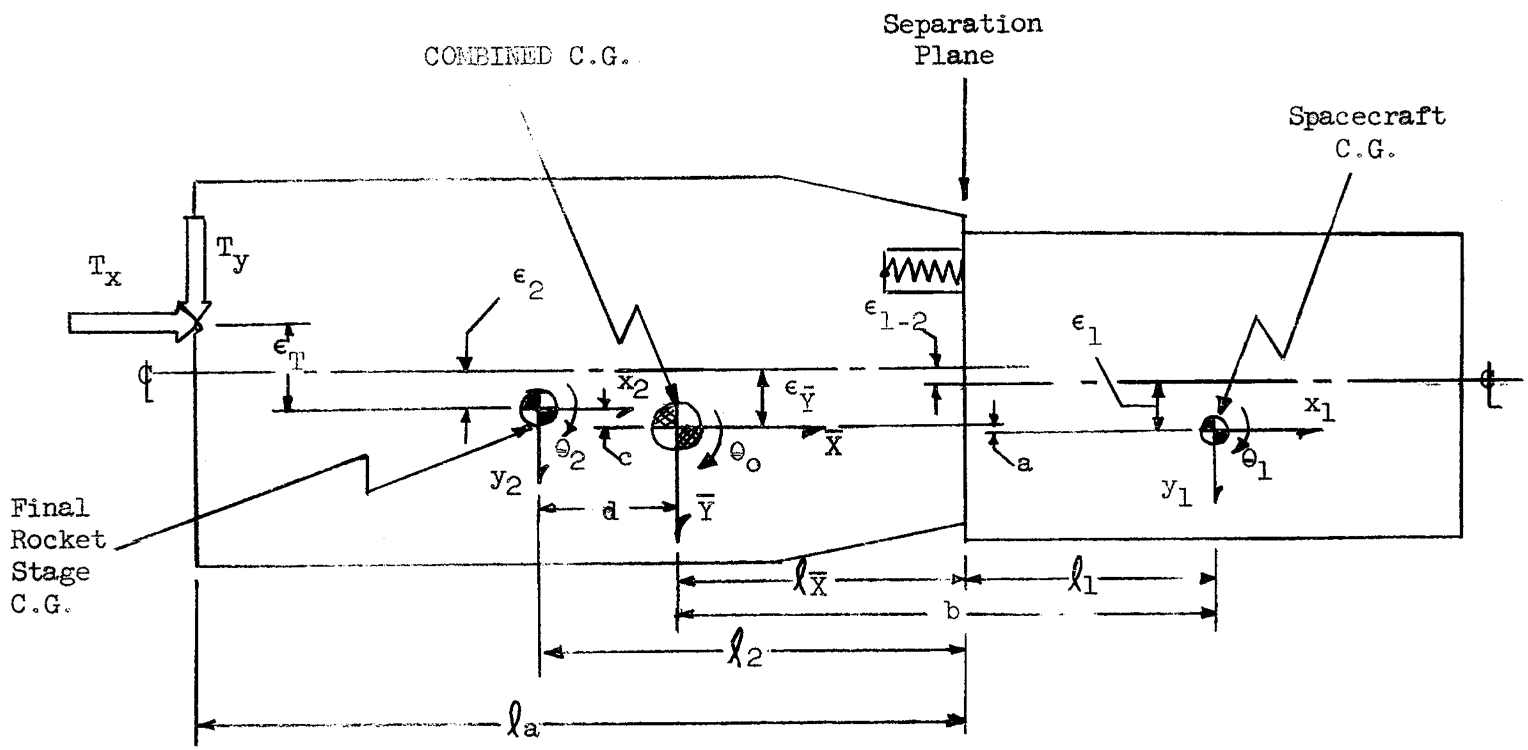

Figure 1. Dynamic Model With Bodies Mated

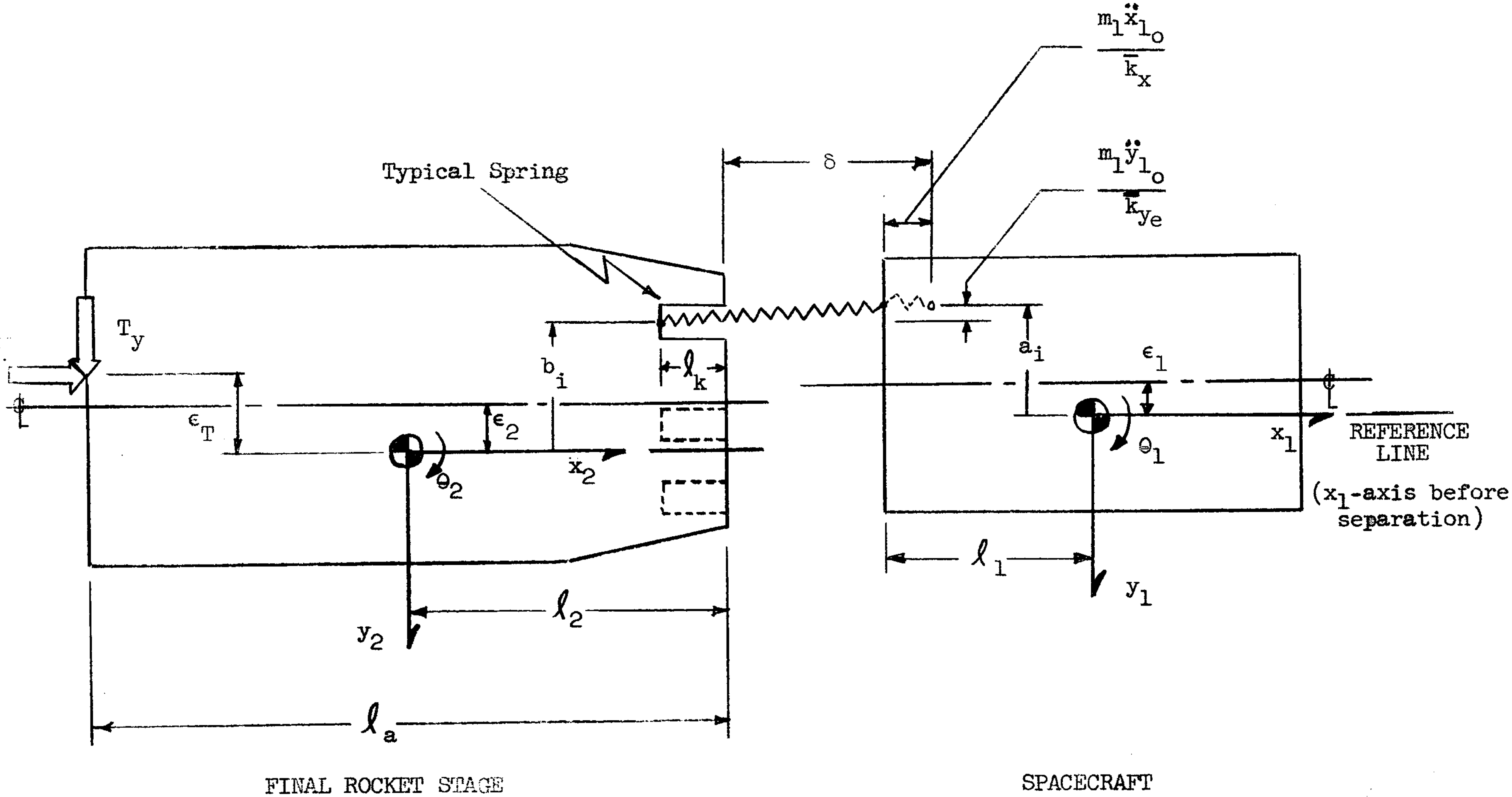

Figure 2. Dynamic Model With Separating Bodies in Equilibrium Position

$$\ell_{\overline{X}} = \left(\frac{m_2}{m_1 + m_2}\right)\ell_2 - \left(\frac{m_1}{m_1 + m_2}\right)\ell_1 \tag{1}$$

where symbols are shown in Figure 1 and defined in Appendix A, List of Symbols.

Doing the same about a point on the final stage centerline to find $\epsilon_{\overline{Y}}$,

$$\epsilon_{\overline{Y}} = \left(\frac{m_2}{m_1 + m_2}\right)\epsilon_2 + \left(\frac{m_1}{m_1 + m_2}\right)\left(\epsilon_1 + \epsilon_{1-2}\right) \tag{2}$$

The composite moment of inertia is equal to the individual moments of inertia of each body plus the transfer terms to the composite center of gravity.

$$I_T = I_1 + I_2 + m_1\left(a^2 + b^2\right) + m_2\left(c^2 + d^2\right) \tag{3}$$

where a, b, c, d are related to the offsets and misalignments shown in Figures 1 and 2 by the relationships

$$a = \epsilon_1 + \epsilon_{1-2} - \epsilon_{\overline{Y}}$$

$$b = \ell_{\overline{X}} + \ell_1$$

$$c = \epsilon_{\overline{Y}} - \epsilon_2$$

$$d = \ell_2 - \ell_{\overline{X}}$$

Looking at the response to the residual thrust, the equations of motion of the combined bodies become

$$\ddot{\overline{X}} = \frac{T_x}{m_1 + m_2} \tag{4a}$$

$$\ddot{\overline{Y}} = \frac{T_y}{m_1 + m_2} \tag{4b}$$

$$\ddot{\theta}_o = \frac{T_x\left(\epsilon_{\overline{Y}} - \epsilon_2 + \epsilon_T\right) - T_y\left(\ell_a - \ell_{\overline{X}}\right)}{I_T} \tag{4c}$$

where $\overline{X}$, $\overline{Y}$, and θ_o are measured from inertial coordinates.

At the time of separation the expression for the complete acceleration of the individual body cg will contain four terms (due to linear, tangential, centripetal and coriolis acceleration terms). This is discussed in Appendix B. However, since the radius to these points is fixed at that time and the angular rotation rate is usually small, only the linear and tangential are significant. Therefore, as shown in Appendix B, the initial linear and angular accelerations of the two bodies shown in Figure 1 can be written as:

Body 1 (Spacecraft)

$$\ddot{x}_{1_o} = \ddot{\bar{X}} - a\ddot{\theta}_o \tag{5a}$$

$$\ddot{y}_{1_o} = \ddot{\bar{Y}} + b\ddot{\theta}_o \tag{5b}$$

$$\ddot{\theta}_{1_o} = \ddot{\theta}_o \tag{5c}$$

Body 2 (Final Stage)

$$\ddot{x}_{2_o} = \ddot{\bar{X}} + c\ddot{\theta}_o \tag{6a}$$

$$\ddot{y}_{2_o} = \ddot{\bar{Y}} - d\ddot{\theta}_o \tag{6b}$$

$$\ddot{\theta}_{2_o} = \ddot{\theta}_o \tag{6c}$$

where these coordinates are also measured from an inertial reference.

Substituting terms from Equations (4), the initial linear and rotational accelerations of each body due to residual thrust become

$$\ddot{x}_{1_o} = \frac{T_x}{m_1 + m_2} - \left[\left(\frac{m_2}{m_1 + m_2}\right)\left(\epsilon_1 + \epsilon_{1-2} - \epsilon_2\right)\right]\ddot{\theta}_o \tag{7a}$$

$$\ddot{y}_{1_o} = \frac{T_y}{m_1 + m_2} + \left[\left(\frac{m_2}{m_1 + m_2}\right)\left(\ell_1 + \ell_2\right)\right]\ddot{\theta}_o \tag{7b}$$

$$\ddot{x}_{2_o} = \frac{T_x}{m_1 + m_2} + \left[\left(\frac{m_1}{m_1 + m_2}\right)\left(\epsilon_1 + \epsilon_{1-2} - \epsilon_2\right)\right]\ddot{\theta}_o \tag{8a}$$

$$\ddot{y}_{2_o} = \frac{T_y}{m_1 + m_2} - \left[\left(\frac{m_1}{m_1 + m_2}\right)\left(\ell_1 + \ell_2\right)\right]\ddot{\theta}_o \tag{8b}$$

and

$$\ddot{\theta}_{1_o} = \ddot{\theta}_{2_o} = \ddot{\theta}_o$$

$$= \frac{T_x\left[m_1\,(\epsilon_1 - \epsilon_2 + \epsilon_{1-2} + \epsilon_T) + m_2\epsilon_T\right] - T_y\left[m_1(\ell_a + \ell_1) + m_2(\ell_a - \ell_2)\right]}{(m_1 + m_2)\,I_T} \tag{9}$$

4. BASIC EQUATIONS OF MOTION DURING SEPARATION

4.1 Spacecraft

A free-body diagram of the spacecraft, Body 1, during separation is shown in Figure 3a. Both external and D'Alembert forces are included. As can be seen, the only external forces acting on the body are those from the separation springs. Only the i^{th} spring is shown but the program has a capability of handling forces from up to four springs.

Since the coordinate system of each body is defined from the "equilibrium" position, which is accelerating, a corrective term must be included in the equations of motion. (i. e., F = ma only in inertial coordinates and the coordinate system of each body is accelerating.) Therefore, the three equations of motion for the spacecraft, Body 1, become

$$m_1\left(\ddot{x}_1 + \ddot{x}_{1_o}\right) - \sum F_{x_i} = 0 \tag{10a}$$

$$m_1\left(\ddot{y}_1 + \ddot{y}_{1_o}\right) - \sum F_{y_i} = 0 \tag{10b}$$

$$I_1\left(\ddot{\theta}_1 + \ddot{\theta}_{1_o}\right) - \sum F_{x_i} a_i + \ell_1 \sum F_{y_i} = 0 \tag{10c}$$

where x_1, y_1 and θ_1 form the accelerating spacecraft coordinate system with its origin at the equilibrium position, all summations are from i = 1 to i = 4 and F_{x_i} and F_{y_i} are the two individual spring force components. Also, since the body coordinate system is rotating, $\ddot{x}_{1_o}$ and $\ddot{y}_{1_o}$, which are derived from an inertial reference, actually have components along both the x_1 and y_1 axes which depend on the angle of rotation θ_1. However,

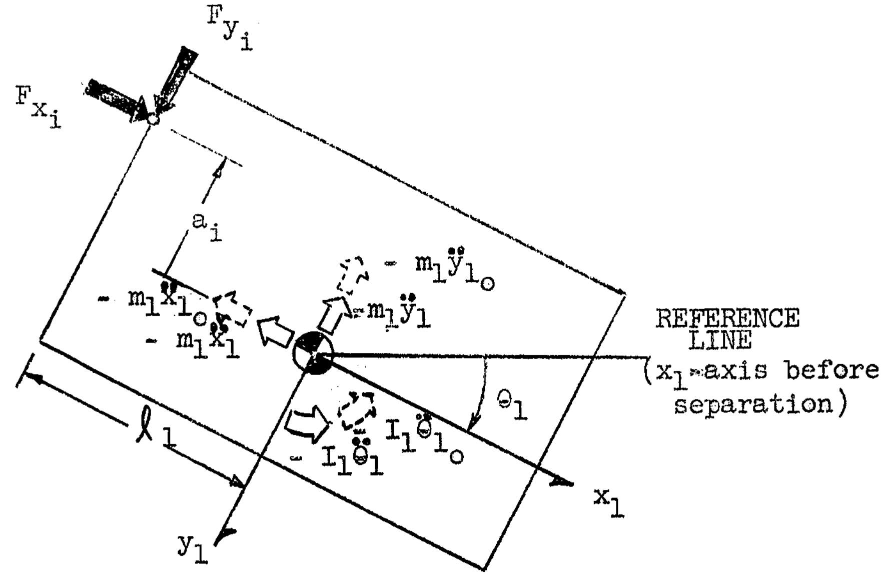

Figure 3a. Spacecraft Free-Body Diagram

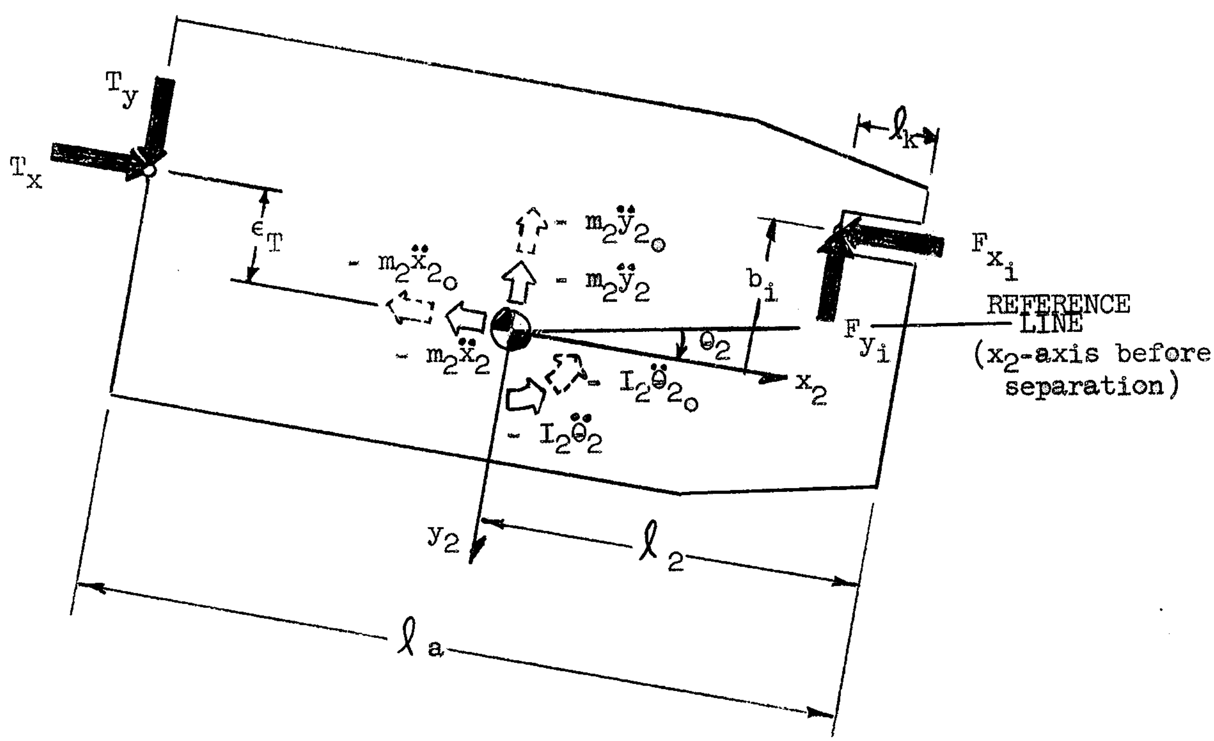

Figure 3b. Final Rocket Stage Free-Body Diagram

during the typical separation θ_1 is always much less than 1 deg. Therefore, these corrective terms are very small and have been neglected.

4.2 Final Rocket Stage

The free-body diagram of the final rocket stage, Body 2, is shown in Figure 3b. Once again both external and D'Alembert forces are included. Here the external forces acting on the body are both the separation spring forces and the residual thrust forces.

With the same assumptions on corrective terms as for the spacecraft, the equations of motion for Body 2 are:

$$m_2\left(\ddot{x}_2 + \ddot{x}_{2_o}\right) + \sum F_{x_i} - T_x = 0 \tag{11a}$$

$$m_2\left(\ddot{y}_2 + \ddot{y}_{2_o}\right) + \sum F_{y_i} - T_y = 0 \tag{11b}$$

$$I_2\left(\ddot{\theta}_2 + \ddot{\theta}_{2_o}\right) + \sum F_{x_i} b_i + \left(\ell_2 - \ell_k\right) \sum F_{y_i} - T_x \epsilon_T + T_y\left(\ell_a - \ell_2\right) = 0 \tag{11c}$$

where F_{x_i} and F_{y_i} are the same as previously defined but in the directions shown in Figure 3b.

5. SPRING FORCES

5.1 Axial Spring Force

It has been found by experience at STL that the forces and moments produced by a helical spring with ends parallel and coaxial as it is compressed along the spring axis are accurately defined by a force vector through the center of the spring and inclined slightly to the spring axis plus a moment about the spring axis. This is discussed in Reference 1.

For both the OGO and 823 programs techniques were developed for matching and pairing springs to compensate for both the lateral component of the force and the moment. Therefore, the separation program assumes that the spring force resulting from an axial compression of each spring lies along the spring axis. While this is not precisely true for each spring the matching process and typical symmetric location of springs in the separation plane will mean that the resulting torques and forces on the two bodies due to these two non-ideal phenomena will cancel out. Therefore, using only the axial force component in the model is sufficient.

Most helical springs used for separation have a nearly linear axial spring rate. This means that the axial spring force is directly proportional and opposite in direction to the axial displacement. The proportionality constant, the axial spring rate, can be calculated for a given helical compression spring design (see Reference 2) or easily measured once the springs have been wound. It has also been found that the axial spring rate is virtually independent of the lateral deflection of the spring, especially for the small lateral deflections that occur during the brief separation time. Therefore, the amplitude of the individual axial spring forces, F_{x_i}, can be represented as

$$F_{x_i} = -k_{x_i} \beta_{x_i} \tag{12}$$

where k_{x_i} is the individual axial spring rate and β_{x_i} is the deflection of the i^{th} spring. The direction of F_{x_i} is shown in Figures 3a and 3b and the deflection of a given spring is defined as

$$\beta_{x_i} = \left(x_1 - x_2\right) + \left(\theta_1 a_i - \theta_2 b_i\right) - \left(\frac{m_1 \ddot{x}_{1_o}}{\bar{k}_x}\right) \tag{13}$$

where the final term corrects for the difference between the origin of the axis system and the free spring length.

The axial spring rate, k_{x_i}, is only defined for compression of the spring (the spring supports no tension loads since it is not attached to the spacecraft). Therefore, $F_{x_i} = 0$ when β_{x_i} is positive.

It should be noted that certain approximations have been made concerning the forces due to the separation springs in this model:

a) The two body-coordinate systems are accelerating and rotating so there should be corrective terms in the expression for each spring deflection. Since the deflection is proportional to the relative displacement between the two bodies, however, these corrective terms are not only small but tend to cancel each other.

b) The x_1 and x_2 axes, and hence the F_{x_i} forces on either end of the spring, are not parallel in this model. The errors involved, however, are higher order since the relative angle $(\theta_1 - \theta_2)$ is small.

c) There is actually a small moment produced by a spring when its opposite ends are not parallel $(\theta_1 \neq \theta_2)$ which has been neglected.

There is no complete rigorous analysis of the forces and moments produced by a helical compression spring for various combinations of compression, lateral deflection, twisting, etc., to include higher order effects. Therefore, detailed definition of the separation spring forces does not seem warranted for this type of analysis.

5.2 Lateral Spring Force

The lateral spring rate (lb/in) of a helical spring is a strong function of the axial deflection, but for a given axial deflection the lateral spring rate is constant. Therefore,

$$F_{y_i} = -k_{y_i} \beta_{y_i} \tag{14}$$

$$\beta_{y_i} = (y_1 - y_2) - \theta_1 \ell_1 - \theta_2 (\ell_2 - \ell_k) - \left(\frac{m_1 \ddot{y}_{1_o}}{\bar{k}_{y_e}} \right) \tag{15}$$

where k_{y_i} is a function of β_{x_i}, and the subsubscript e denotes the value at equilibrium. The direction of F_{y_i} is shown in Figures 3a and 3b.

The precise relationship between the lateral spring rate and the axial deflection for a helical compression spring has not been proven. Theoretical approaches (Reference 3 and 4) indicate that the lateral rate decreases as the axial deflection increases. Experience at STL, however, indicates that for the type of springs used in the OGO and 823 separation systems the lateral spring rate actually increases as the axial deflection increases. This is also discussed in Reference 1. In either case, the relationship between k_{y_i} and β_{x_i} is not linear. For that reason, the separation program provides for a table of values of k_{y_i} versus β_{x_i} for each spring.

The axial force of the spring will be zero at the instant it separates, since it will not support tension. However, there may be a lateral spring deflection, and hence a lateral load, right up to separation. In fact, the spring will give a lateral force even after the free height of the spring is reached, until the lip of the separation spring cup on the satellite is cleared. Therefore, k_{y_i} is defined from the given table until $\beta_{x_i} = \delta_w$, the width of this lip, and then $k_{y_i} = 0$ for greater values of β_{x_i}.

6. SOLUTION OF EQUATIONS OF MOTION

At any given time during separation each spring will be in one of three conditions:

a) Transmitting both lateral and longitudinal spring forces ($\beta_{x_i} < 0$)

b) Transmitting a lateral spring force only ($0 \leq \beta_{x_i} \leq \delta_w$)

c) Completely detached from spacecraft ($\beta_{x_i} > \delta_w$)

Since each spring can move from one condition to another at different times the only two states where the complete equations of motion can be written in fairly simplified terms are:

a) Before any spring reaches its free length

b) After all springs have detached.

During the intermediate condition there will be some springs in each of the three combinations (a, b, or c).

In the first state the equations of motion become by substitution of Equations (12), (13), (14), and (15) into Equations (10) and (11)

STATE I (All Springs Compressed)

Body 1 (Spacecraft)

$$\ddot{x}_1 + \left[\frac{\bar{k}_x}{m_1}\right] x_1 = \left[\frac{\bar{k}_x}{m_1}\right] x_2 - \left[\sum \frac{k_{x_i} a_i}{m_1}\right] \theta_1 + \left[\sum \frac{k_{x_i} b_i}{m_1}\right] \theta_2 \tag{16a}$$

$$\ddot{y}_1 + \left[\frac{\bar{k}_y}{m_1}\right] y_1 = \left[\frac{\bar{k}_y}{m_1}\right] y_2 + \left[\frac{\bar{k}_y \ell_1}{m_1}\right] \theta_1 + \left[\frac{\bar{k}_y(\ell_2 - \ell_k)}{m_1}\right] \theta_2 + \ddot{y}_{1_o} \left[\frac{\bar{k}_y}{\bar{k}_{y_e}} - 1\right] \tag{16b}$$

$$\ddot{\theta}_1 + \left[\frac{\sum k_{x_i}(a_i)^2 + \bar{k}_y \ell_1^{\,2}}{I_1}\right]\theta_1$$

$$= \left[\frac{\sum k_{x_i} a_i b_i - \bar{k}_y \ell_1 (\ell_2 - \ell_k)}{I_1}\right]\theta_2 - \left[\sum \frac{k_{x_i} a_i}{I_1}\right] x_1$$

$$+ \left[\sum \frac{k_{x_i} a_i}{I_1}\right] x_2 + \left[\frac{\bar{k}_y \ell_1}{I_1}\right] y_1 - \left[\frac{\bar{k}_y \ell_1}{I_1}\right] y_2 - A_o \tag{16c}$$

Body 2 (Final Rocket Stage)

$$\ddot{x}_2 + \left[\frac{\bar{k}_x}{m_2}\right] x_2 = \left[\frac{\bar{k}_x}{m_2}\right] x_1 + \left[\sum \frac{k_{x_i} a_i}{m_2}\right]\theta_1 - \left[\sum \frac{k_{x_i} b_i}{m_2}\right]\theta_2 \tag{17a}$$

$$\ddot{y}_2 + \left[\frac{\bar{k}_y}{m_2}\right] y_2 = \left[\frac{\bar{k}_y}{m_2}\right] y_1 - \left[\frac{\bar{k}_y \ell_1}{m_2}\right]\theta_1 - \left[\frac{\bar{k}_y(\ell_2 - \ell_k)}{m_2}\right]\theta_2 + \left[\ddot{y}_{2_o} - \frac{T_y}{m_2}\right]\left[\frac{\bar{k}_y}{\bar{k}_{y_e}} - 1\right] \tag{17b}$$

$$\ddot{\theta}_2 + \left[\frac{\sum k_{x_i}(b_i)^2 + \bar{k}_y(\ell_2 - \ell_k)^2}{I_2}\right]\theta_2$$

$$= \left[\frac{\sum k_{x_i} a_i b_i - \bar{k}_y \ell_1 (\ell_2 - \ell_k)}{I_2}\right]\theta_1 + \left[\sum \frac{k_{x_i} b_i}{I_2}\right] x_1$$

$$- \left[\sum \frac{k_{x_i} b_i}{I_2}\right] x_2 + \left[\frac{\bar{k}_y(\ell_2 - \ell_k)}{I_2}\right] y_1$$

$$- \left[\frac{\bar{k}_y(\ell_2 - \ell_k)}{I_2}\right] y_2 - C_o \tag{17c}$$

where all summations are from i = 1 to i = 4 and

$$A_o = \ddot{\theta}_{1_o} - \frac{m_1 \ddot{x}_{1_o}}{I_1 \bar{k}_x} \sum k_{x_i} a_i + \frac{m_1 \ddot{y}_{1_o} \ell_1 \bar{k}_y}{I_1 \bar{k}_{y_e}}$$

$$C_o = \ddot{\theta}_{2_o} + \frac{m_1 \ddot{x}_{1_o}}{I_2 \bar{k}_x} \sum k_{x_i} b_i + \frac{m_1 \ddot{y}_{1_o} \bar{k}_y}{I_2 \bar{k}_{y_e}} \left(\ell_2 - \ell_k\right) - \frac{T_x \epsilon_T}{I_2} + \frac{T_y}{I_2} \left(\ell_a - \ell_2\right)$$

In the intermediate state, State II, all the lateral spring force terms, those containing $\bar{k}_y$, will be the same as for State I, but only the axial spring force terms from springs still in contact will be present. Therefore, the equations are the same for State II as for State I except that the summations are only over the values of i where $\beta_{x_i} < 0$.

For the final state, State III, all the spring force terms, from Equations (10) and (11) drop out, and the equations of motion become

STATE III (All Springs Detached, Complete Separation)

Body 1 (Spacecraft)

$$\ddot{x}_1 = -\ddot{x}_{1_o} \tag{18a}$$

$$\ddot{y}_1 = -\ddot{y}_{1_o} \tag{18b}$$

$$\ddot{\theta}_1 = -\ddot{\theta}_{1_o} \tag{18c}$$

Body 2 (Final Rocket Stage)

$$\ddot{x}_2 = \frac{T_x}{m_2} - \ddot{x}_{2_o} \tag{19a}$$

$$\ddot{y}_2 = \frac{T_y}{m_2} - \ddot{y}_{2_o} \tag{19b}$$

$$\ddot{\theta}_2 = \frac{T_x \epsilon_T}{I_2} - \frac{T_y\left(\ell_a - \ell_2\right)}{I_2} - \ddot{\theta}_{2_o} \tag{19c}$$

When the separation is complete the spacecraft has no external forces acting on it and hence no acceleration with respect to inertial space. Therefore, the acceleration components in the accelerating coordinate system are equal and opposite to the corresponding inertial accelerations of the reference system.

The final rocket stage is still accelerating due to the residual thrust. However, the acceleration is different from that of the reference system since the mass acted upon by the force is now only m_2 instead of $m_1 + m_2$ and the cg is now the body's cg, rather than the combined center of gravity. The right-hand terms in Equations (19) correct for these changes.

7. COMPUTER SOLUTION

The six basic equations of motion for the two bodies in State I, Equations (16) and Equations (17), have been programmed for solution on the IBM 7090 digital computer. The equations for States II and III are actually special cases of those for State I so these equations cover the complete separation regime. Every axial spring deflection is examined during each integration step to determine which terms of the summation should be included and which should be dropped. Therefore, the equations used for calculation transfer automatically from those of State I, through State II, to those of State III as the spring terms vanish.

Provision is made in the program for any arbitrary initial conditions of the various parameters. Care must be taken, however, to stay with the ranges where the solutions are accurate, as discussed previously.

The initial values of certain parameters are set by the assumptions used or by geometric constraints. The initial accelerations, velocities and displacements are constrained as follows:

7.1 Initial Accelerations

The initial accelerations in inertial coordinates

$$\left(\ddot{x}_{1_o}, \ddot{x}_{2_o}, \ddot{y}_{1_o}, \ddot{y}_{2_o}, \ddot{\theta}_{1_o}, \text{ and } \ddot{\theta}_{2_o}\right)$$

have been derived previously [Equations (5) and (6)]. The initial accelerations in the body-coordinates should be zero since the bodies are clamped together initially.

7.2 Initial Velocities

The initial velocities of each body in inertial coordinates are determined by the geometric relationships

$$\dot{x}_{1_o} = \dot{\bar{X}} - a\dot{\theta}_o$$

$$\dot{x}_{2_o} = \dot{\bar{X}} + c\dot{\theta}_o$$

$$\dot{y}_{1_o} = \dot{\bar{Y}} + b\dot{\theta}_o$$

$$\dot{y}_{2_o} = \dot{\bar{Y}} - d\dot{\theta}_o$$

$$\dot{\theta}_{1_o} = \dot{\theta}_{2_o} = \dot{\theta}_o$$

where $\dot{\bar{X}}$, $\dot{\bar{Y}}$ and $\dot{\theta}_o$ are arbitrary. The body-coordinate velocities should be zero initially.

7.3 Initial Displacements

The initial displacements in body coordinates

$$x_{1_o},\ x_{2_o},\ y_{1_o},\ \text{and } y_{2_o}$$

are related by the compressed length of the spring and initial offsets

$$x_{1_o} = \frac{m_1 \ddot{x}_{1_o}}{\bar{k}_x} - \delta + x_{2_o}$$

$$y_{1_o} = \frac{m_1 \ddot{y}_{1_o}}{\bar{k}_y} + \epsilon_{k_o} + y_{2_o}$$

where the average initial lateral offset, ϵ_{k_o}, is defined by

$$\epsilon_{k_o} = \epsilon_1 - \epsilon_2 + \epsilon_{1-2} - 1/4 \left[\sum a_i - \sum b_i\right]$$

and the summations are from i = 1 to 4.

7.4 Initial Rotations

The initial rotations, θ_{1_o} and θ_{2_o}, are equal since the bodies are clamped together before separation.

8. INPUT AND OUTPUT OF COMPUTER

8.1 Input

For a particular problem the following parameters must be provided:

$$\left.\begin{array}{llllllll} \epsilon_1 & \ell_1 & I_1 & T_x & a_1 & b_1 & k_{x_1} & k_{y_1} \\ \epsilon_2 & \ell_2 & I_2 & T_y & a_2 & b_2 & k_{x_2} & k_{y_2} \\ \epsilon_{1-2} & \ell_a & m_1 & \delta & a_3 & b_3 & k_{x_3} & k_{y_3} \\ \epsilon_T & \ell_k & m_2 & \delta_w & a_4 & b_4 & k_{x_4} & k_{y_4} \end{array}\right\} \begin{array}{c}\text{Either as a constant}\\ \text{or as a table versus}\\ \beta_{x_i}\end{array}$$

The following parameters can either be provided or will be calculated by the program:

ϵ_{k_o} $\quad I_T \quad$ Initial Conditions (See Section 7)

Copies of the actual 7090 Symbolic Code Form, showing the method of input, are shown in Figures 4a and 4b.

The program (CDRC Problem No. 3682), as written, assumes that $\delta_w = 0.5$ inch. If other values of spring cup width are desired it must be changed in the program.

The form used for the tables of lateral spring rates is:

$$(\text{Beta})_1, \ (k_y)_1, \ (\text{Beta})_2, \ (k_y)_2, \ \text{etc.},$$

where subscripts pertain to increasing values of Beta-X_i.

All numbers in the input must have decimal points, including the numbers which indicate how many pairs of values are given in the Beta versus k_y tables.

Since δ_w has been programmed in inches, all lengths should be input in inches. Other dimensions are arbitrary as long as they are consistent.

7090 SYMBOLIC CODING FORM

SPACE TECHNOLOGY LABORATORIES
COMPUTATION AND DATA REDUCTION CENTER

TO BE FILLED IN BY DISPATCHER	TO BE FILLED IN BY PROGRAMMER	DATE	PAGE 1 OF 2
SEQUENCE NO. ____ (2-5)	PROGRAMMER'S NAME (LAST NAME FIRST) ____ (18-29)		
TYPE OF SERVICE 59 (6-7)	PROBLEM NO. 3682 (30-35)	KEYPUNCHED BY ____ (43-45)	VERIFIED BY ____ (58-60)
DATE OF REQUEST (MO-DAY-YR) ____ (8-13)	PRIORITY NOMINAL 3 (36) ACTUAL ____ (37-38)	DATE ____ (46-49)	DATE ____ (61-64)
TIME SUBMITTED ____ (14-17)	NO. OF CARDS ____ (39-42)	TIME ____ (50-57)	TIME ____ (65-72)

LOCATION 1 6	OPERATION 8 14	ADDRESS, TAG, DECREMENT/COUNT 16	COMMENTS 34 72	LABEL 73 80
SID	BCI 1, 5	CASE 1 NØ. 1	Identification of Problem	
SDELTA	DEC		δ	
SEPS1			ϵ_1	
SEPS2			ϵ_2	
SEPS12			ϵ_{1-2}	
SEPSKØ			ϵ_{k_o} (put "0" here and program will compute value)	
SA1			a_1	
SA2			a_2	
SA3			a_3	
SA4			a_4	
SB1			b_1	
SB2			b_2	
SB3			b_3	
SB4			b_4	
SEPST			ϵ_T	
SI1			I_1	
SI2			I_2	
SITRD			I_T (put "0" here and program will compute value)	
SKX1			k_{x_1}	
SKX2			k_{x_2}	
SKX3			k_{x_3}	
SKX4			k_{x_4}	
SKY1			k_{y_1} (if in a table, put "0" here)	
SKY2			k_{y_2} (if in a table, put "0" here)	
SKY3	DEC		k_{y_3} (if in a table, put "0" here)	

* in column 1 indicates comment card; comment may start in any field; column 2, 7, 8, 15, 16 or 34.

STL FORM 1149 REV. 9/61

69

Figure 4a. 7090 Symbolic Coding Form for Separation Program
(Page 1 of 2)

7090 SYMBOLIC CODING FORM

SPACE TECHNOLOGY LABORATORIES
COMPUTATION AND DATA REDUCTION CENTER

TO BE FILLED IN BY DISPATCHER	TO BE FILLED IN BY PROGRAMMER	DATE	PAGE 2 OF 2
SEQUENCE NO. ______ (2-5)	PROGRAMMER'S NAME (LAST NAME FIRST) ______ (18-29)	KEYPUNCHED BY ______ (43-45)	VERIFIED BY ______ (58-60)
TYPE OF SERVICE S9 (6-7)	PROBLEM NO. ______ (30-35)	DATE ______ (46-49)	DATE ______ (61-64)
DATE OF REQUEST (MO DAY YR) ______ (8-13)	PRIORITY: NOMINAL ______ (36) ACTUAL ______ (37-38)	TIME ______ (50-57)	TIME ______ (65-72)
TIME SUBMITTED ______ (14-17)	NO. OF CARDS ______ (39-42)		

LOCATION 1–6	OPERATION 8–14	ADDRESS, TAG, DECREMENT/COUNT 16	COMMENTS 34–72	LABEL 73–80
SKY4	DEC		$^{k}y_4$ (if in a table, put "0" here)	
SL1	↑		ℓ_1	
SL2			ℓ_2	
SLA			ℓ_a	
SLK			ℓ_K	
SM1			m_1	
SM2			m_2	
SSTEPI			Starting Integration Step Size	
STSTØP			Maximum Value of Time for Solution	
STX			T_X	
STY			T_Y	
STABY1			Table - Beta-X_1 vs. $^{k}y_1$	
			Additional card(s) for table	
STABY2			Table - Beta-X_2 vs. $^{k}y_2$	
			Additional card(s) for table	
STABY3			Table - Beta-X_3 vs. $^{k}y_3$	
			Additional card(s) for table	
STABY4			Table - Beta-X_4 vs. $^{k}y_4$	
			Additional card(s) for table	
SPXY1			No. pairs of Beta-X_1 vs. $^{k}y_1$	
SPXY2			No. pairs of Beta-X_2 vs. $^{k}y_2$	
SPXY3	↓		No. pairs of Beta-X_3 vs. $^{k}y_3$	
SPXY4	DEC		No. pairs of Beta-X_4 vs. $^{k}y_4$	
S	TRA	SYMTR		

* in column 1 indicates comment card; comment may start in any field: column 2, 7, 8, 15, 16 or 34.

STL FORM 1149 REV. 9/61

Figure 4b. 7090 Symbolic Coding Form for Separation Program (Page 2 of 2)

8.2 Output

The printout of the program will provide, for each integration step, the following:

Time	x_1	x_2	y_1	y_2	θ_1	θ_2	$\bar{X}$	$\bar{Y}$	θ_o
	$\dot{x}_1$	$\dot{x}_2$	$\dot{y}_1$	$\dot{y}_2$	$\dot{\theta}_1$	$\dot{\theta}_2$	$\dot{\bar{X}}$	$\dot{\bar{Y}}$	$\dot{\theta}_o$
	$\ddot{x}_1$	$\ddot{x}_2$	$\ddot{y}_1$	$\ddot{y}_2$	$\ddot{\theta}_1$	$\ddot{\theta}_2$	$\ddot{\bar{X}}$	$\ddot{\bar{Y}}$	$\ddot{\theta}_o$

All angles are given both in terms of radians and arc degrees.

8.3 Example Problem

The following example problem illustrates the type of solution available with this separation program. For this example the input values are:

δ = 2.08 inch	a_1 = 8.642 inch
ϵ_1 = 0.092 inch	a_2 = 0.097 inch
ϵ_2 = 0.316 inch	a_3 = -8.448 inch
ϵ_{1-2} = 0	a_4 = 0.097 inch
ϵ_T = 0	b_1 = 8.866 inch
T_X = 0	b_2 = 0.321 inch
T_Y = 0	b_3 = -8.224 inch
I_1 = 2330 lb-sec^2-in	b_4 = 0.321 inch
I_2 = 24,900 lb-sec^2-in	$k_{x_1} = k_{x_2} = k_{x_3} = k_{x_4}$ = 55 lb/in
ℓ_1 = 47.625 inch	m_1 = 2.695 lb-sec^2/in
ℓ_2 = 133.8 inch	m_2 = 3.918 lb-sec^2/in
ℓ_k = 1.14 inch	

For all springs the following table of k_{y_i} versus β_{x_i} is used:

β_{x_i} (inch)	k_{y_i} (lb/in)
-2.08	47.2
-1.83	37.4
-1.58	30.0
-1.08	22.4
-0.83	20.2
-0.58	20.0
-0.33	21.0
-0	26.0
+0.5	26.0

The values of θ_1, $\dot{\theta}_1$, θ_2, $\dot{\theta}_2$, and $(\dot{x}_1 - \dot{x}_2)$ are shown versus time as the bodies separate in Figure 5.

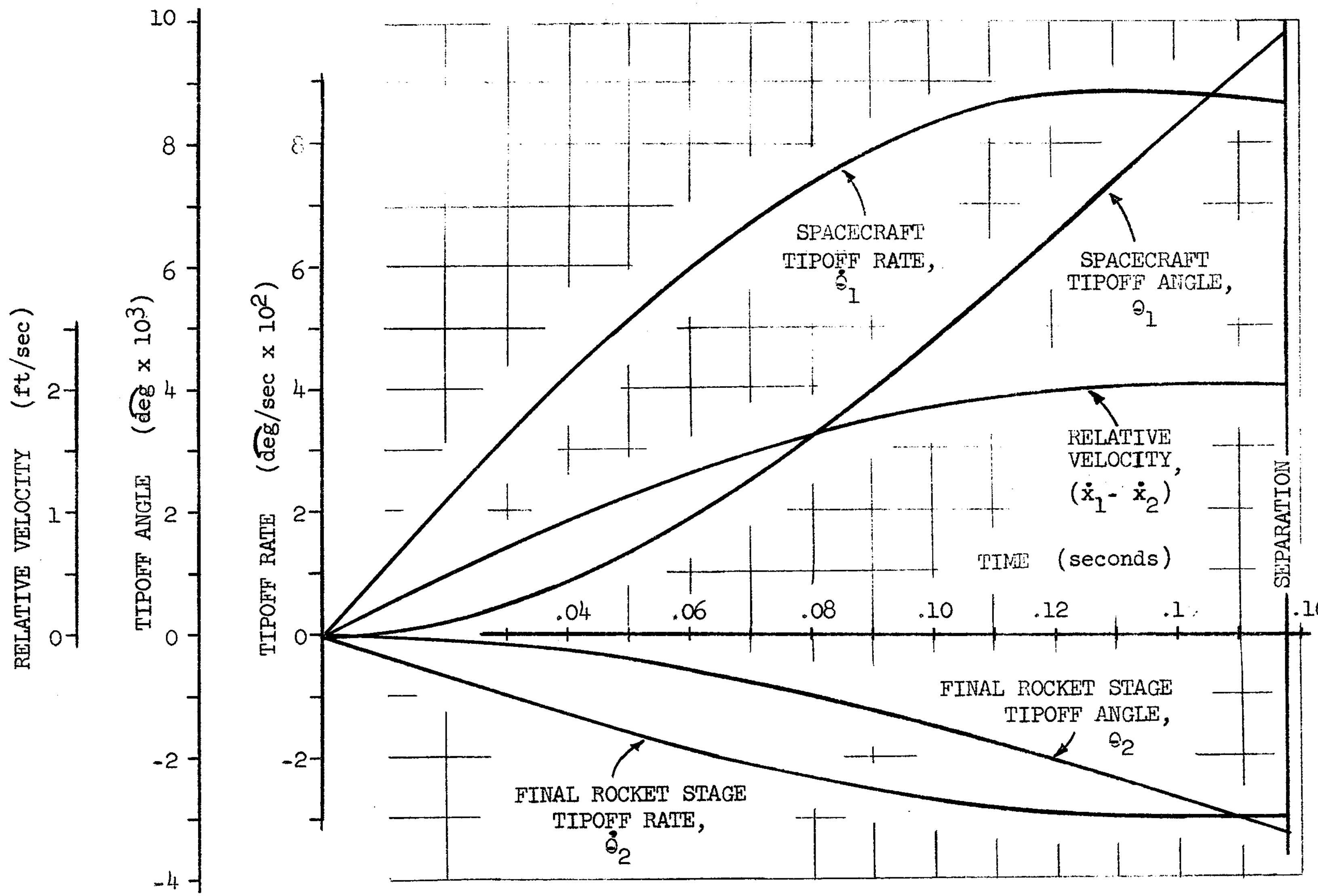

Figure 5. Example Problem

APPENDIX A

LIST OF SYMBOLS

a_i	Lateral displacement of i^{th} spring attach point from spacecraft center of gravity (see Figure 2) (inch)
b_i	Lateral displacement of i^{th} spring attach point from final stage cg (see Figure 2) (inch)
I_1	Moment of inertia of spacecraft about its cg (lb-sec^2-in)
I_2	Moment of inertia of final stage about its cg (lb-sec^2-in)
I_T	Total moment of inertia of mated bodies about the combined cg (lb-sec^2-in)
k_{x_i}	Longitudinal spring rate of i^{th} separation spring (lb/in)
k_{y_i}	Lateral spring rate of i^{th} separation spring (lb/in)
$\overline{k}_x$	Total longitudinal spring rate of separation springs $\left(k_{x_1} + k_{x_2} + k_{x_3} + k_{x_4}\right)$ (lb/in)
$\overline{k}_y$	Total lateral spring rate of separation springs $\left(k_{y_1} + k_{y_2} + k_{y_3} + k_{y_4}\right)$ (lb/in)
ℓ_1	Location of spacecraft cg with respect to separation plane (see Figure 1) (inch)
ℓ_2	Location of final stage cg with respect to separation plane (see Figure 1) (inch)
ℓ_a	Length of final stage (see Figure 1) (inch)
ℓ_k	Compressed height of separation spring (see Figure 1) (inch)
$\ell_{\overline{X}}$	Location of combined cg with respect to separation plane (see Figure 1) (inch)
m_1	Mass of spacecraft (lb-sec^2/in)
m_2	Mass of final stage (lb-sec^2/in)
T_x	Residual thrust force along x_2 axis (see Figure 1) (pound)
T_y	Residual thrust force along y_2 axis (see Figure 1) (pound)

x_1, y_1	Displacement components of spacecraft from equilibirum position (see Figure 2) (inch) (Accelerating and rotating reference)
x_2, y_2	Displacement components of final stage from equilibrium position (see Figure 2) (inch) (Accelerating and rotating reference)
$\overline{X}, \overline{Y}$	Displacement components of mated bodies (see Figure 1) (inch) (Inertial reference)
β_{x_i}	Axial deflection of i^{th} spring (inch) [see Equation (14)]
β_{y_i}	Lateral deflection of i^{th} spring (inch) [see Equation (16)]
δ	Stroke length of all separation springs (see Figure 2) (inch)
δ_w	Width of lip on separation spring cups (inch)
ϵ_1	Lateral displacement of spacecraft cg with respect to its centerline (see Figure 1) (inch)
ϵ_2	Lateral displacement of final stage cg with respect to its centerline (see Figure 1) (inch)
ϵ_{1-2}	Lateral misalignment of two centerlines (see Figure 1) (inch)
ϵ_T	Lateral displacement of T_x from final stage cg (see Figure 1) (inch)
$\epsilon_{\overline{Y}}$	Lateral displacement of combined cg from final stage centerline (see Figure 1) (inch)
θ_1, θ_2	Angular rotation of spacecraft and final stage, respectively, about its own cg (rad or deg) (Accelerating and rotating references)
θ_o	Angular rotation of mated bodies about the combined cg (rad or deg) (Inertial reference)
N. B.	Superscript dots denote time derivatives. Subsubscripts "o" denote initial, mated-body conditions. Subsubscripts "e" denote conditions when bodies are in the equilibrium position.

APPENDIX B

TOTAL ACCELERATION OF A POINT NOT AT THE CENTER OF GRAVITY

The problem of finding the initial acceleration components of each separating body is one of coordinate tranformations.

Consider first the coordinates of the mated bodies, $\overline{X}$, $\overline{Y}$, and θ_o. The reference of this system is a point in inertial space. The acceleration components of the combined cg with respect to this point, therefore, at any time are precisely equal to $\ddot{\overline{X}}$ along $\overline{X}$, $\ddot{\overline{Y}}$ along $\overline{Y}$ and $\ddot{\theta}_o$ about the $\overline{Z}$-axis, which is normal to the $\overline{X}$-$\overline{Y}$ plane.

The acceleration of any point a distance r from the combined cg with respect to the cg can be written in terms of the radial and tangential acceleration components, a_r and a_T, where a_r is along r and a_T is perpendicular to this. From basic dynamic theory,

$$a_r = \ddot{r} - r\left(\dot{\theta}_o\right)^2 \qquad \text{(B. 1a)}$$

$$a_T = r\ddot{\theta}_o + 2\dot{r}\dot{\theta}_o \qquad \text{(B. 1b)}$$

However, just prior to the instant of release the distance r is constant and its first two derivatives are zero. Therefore

$$a_r = -r\left(\dot{\theta}_o\right)^2 \qquad \text{(B. 2a)}$$

$$a_T = r\ddot{\theta}_o \qquad \text{(B. 2b)}$$

The total inertial acceleration of each cg, in the mated-body axis system, is the sum of these two components, plus the acceleration of the combined center of gravity

$$a_{\overline{X}} = \ddot{\overline{X}} - r\left(\dot{\theta}_o\right)^2 \cos\phi - r\ddot{\theta}_o \sin\phi \qquad \text{(B. 3a)}$$

$$a_{\overline{Y}} = \ddot{\overline{Y}} - r\left(\dot{\theta}_o\right)^2 \sin\phi + r\ddot{\theta}_o \cos\phi \qquad \text{(B. 3b)}$$

$$a_{\theta_o} = \ddot{\theta}_o \qquad \text{(B. 3c)}$$

where ϕ is the angle between r and the $\overline{X}$ axis.

For the two individual bodies, using the distances to the two centers of gravity shown in Figure 1

<u>Spacecraft</u>

$$\left(a_{\bar{X}}\right)_1 = \ddot{x}_{1_o} = \ddot{\bar{X}} - b\left(\dot{\theta}\right)^2 - a\ddot{\theta}_o \qquad \text{(B.4a)}$$

$$\left(a_{\bar{Y}}\right)_1 = \ddot{y}_{1_o} = \ddot{\bar{Y}} - a\left(\dot{\theta}_o\right)^2 + b\ddot{\theta}_o \qquad \text{(B.4b)}$$

$$\left(a_{\theta_o}\right)_1 = \ddot{\theta}_{1_o} = \ddot{\theta}_o \qquad \text{(B.4c)}$$

<u>Final Stage</u>

$$\left(a_{\bar{X}}\right)_2 = \ddot{x}_{2_o} = \ddot{\bar{X}} + d\left(\dot{\theta}_o\right)^2 + c\ddot{\theta}_o \qquad \text{(B.5a)}$$

$$\left(a_{\bar{Y}}\right)_2 = \ddot{y}_{2_o} = \ddot{\bar{Y}} + c\left(\dot{\theta}_o\right)^2 - d\ddot{\theta}_o \qquad \text{(B.5b)}$$

$$\left(a_{\theta_o}\right)_2 = \ddot{\theta}_{2_o} = \ddot{\theta}_o \qquad \text{(B.5c)}$$

For most spacecraft separation problems the angular velocity is small since the final rocket stage usually has an active control system. Therefore, the $\left(\dot{\theta}_o\right)^2$ terms can be neglected. This also has the advantage of leaving only acceleration terms in the calculation of the initial conditions, meaning that they can be found explicitly in terms of the forces and moments acting on the combined bodies. As simplified,

$$\ddot{x}_{1_o} = \ddot{\bar{X}} - a\ddot{\theta}_o \qquad \text{(B.6a)} \qquad\qquad \ddot{x}_{2_o} = \ddot{\bar{X}} + c\ddot{\theta}_o \qquad \text{(B.7a)}$$

$$\ddot{y}_{1_o} = \ddot{\bar{Y}} + b\ddot{\theta}_o \qquad \text{(B.6b)} \qquad\qquad \ddot{y}_{2_o} = \ddot{\bar{Y}} - d\ddot{\theta}_o \qquad \text{(B.7b)}$$

$$\ddot{\theta}_{1_o} = \ddot{\theta}_o \qquad \text{(B.6c)} \qquad\qquad \ddot{\theta}_{2_o} = \ddot{\theta}_o \qquad \text{(B.7c)}$$

These are also Equations (5) and (6) of the main text.

REFERENCES

1. W. E. Smith, "Calibration and Matching of OGO Flight Separation Springs," and Addenda, 9711. 1-73 (5 October 1962), 9711. 1-74 (5 October 1962), and 9711. 1-2 (29 January 1963), Space Technology Laboratories, Inc.

2. Manual of Spring Engineering, American Steel and Wire Division, U. S. Steel Corporation, 1958.

3. C. E. Crede, "Vibration and Shock Isolation," Wiley and Sons (1951), pp. 242-249.

4. A. M. Wahl, "Mechanical Springs," Kent's Mechanical Engineer's Handbook, Chapter 11, pp. 11-02 to 11-19.

DISTRIBUTION

R. M. Acker
W. Aichroth
P. N. Anderson
J. S. Archer
M. V. Barton
M. J. Berg
R. L. Bruckwick (5)
W. J. Chalmers
D. O. Chandler
S. R. Futterman
P. F. Glaser (20)
D. L. Jones
R. F. Lay
T. J. Maxey
F. S. Mosher
E. M. Noneman
T. J. Ockey
C. A. Schorken
J. H. Schroeder
W. B. J. Shakespeare
W. F. Sheehan
W. E. Smith
L. Strauss
A. M. Takemoto
R. C. Turkolu
Dynamics Department